Atomically Resolved Silver Imaging on the Si(111)-($\sqrt{3} \times \sqrt{3}$)-Ag Surface Using a Noncontact Atomic Force Microscope

Kousuke Yokoyama,* Taketoshi Ochi, Yasuhiro Sugawara, and Seizo Morita

Department of Electronic Engineering, Graduate School of Engineering, Osaka University, 2-1 Yamada-Oka, Suita, Osaka 565-0871, Japan

We experimentally investigate the noncontact atomic force microscopy (AFM) imaging on the Si(111)-($\sqrt{3} \times \sqrt{3}$)-Ag surface. An individual silver atom on the topmost layer of the surface can be resolved. The image patterns have no distance dependence, which suggests that the strong chemical-bonding interaction between the tip and the surface does not contribute to image contrast. The silver atom on the surface seems to be resolved with the silver adsorbed tip. This result suggests that the noncontact AFM images drastically change depending on the atom species (e.g., silver or silicon) on the tip apex.

The atomic force microscopy (AFM) has been developed into a novel technique for resolving the atomic features of both conductors and insulators [1]. In contact mode, atomic scale point defects have not been imaged, because a large repulsive force between an AFM tip and a sample surface destroyed the initial sharp tip apex and the sample surface.

However, in the noncontact mode, the destruction of the tip apex and the sample surface can be avoided. In 1995, the noncontact AFM using the frequency modulation (FM) technique achieved true atomic resolution [2–5]. At present, various surfaces such as clean semiconductors [2–9], ionic crystals [10], metal oxide [11], metal deposited semiconductor [12], pure metals [13,14], and layered material [15] have been observed successfully with atomic resolution.

In order to apply the noncontact AFM as a powerful scientific tool for resolving the atomic features in a variety of fields such as materials and biological sciences, it is very important to clarify the imaging mechanism of the noncontact AFM. The imaging mechanism of the noncontact AFM was not clearly established; however, the investigation concerning the imaging mechanism has been making progress gradually on various surfaces.

Recently, on the Si(111)-($\sqrt{3} \times \sqrt{3}$)-Ag surface, we observed three types of AFM image patterns which depend on the distance between the reactive silicon tip and sample surface [12]. Far from the sample surface, the tip-sample interaction seems to be dominated by physical bonding interaction, while just before contact, it seems to be dominated by the chemical bonding interaction due to the onset of the orbital hybridization [12]. This suggests that the noncontact AFM does not reflect the surface topography. However, very recently, we found that, in some cases, the noncontact AFM can resolve an individual silver atom on the topmost layer of the Si(111)-($\sqrt{3} \times \sqrt{3}$)-Ag surface. Hereafter, these

noncontact AFM imaging types of the former and latter are referred to as type-I and type-II, respectively.

In this paper, we present the results of the noncontact AFM imaging, which resolved the individual silver atoms on the Si(111)-($\sqrt{3} \times \sqrt{3}$)-Ag (hereafter referred to as $\sqrt{3}$-Ag) surface, and consider why the image patterns of the noncontact AFM drastically changed from type-I to type-II.

We used the specially designed noncontact AFM with an optical beam deflection detection system operating in ultrahigh vacuum [16]. The FM technique [17] was used to detect the frequency shift $\Delta \nu$ of the cantilever resonance frequency. As the operating mode, the constant excitation mode was used to minimize the destruction of the tip apex and the sample surface, in which the constant amplitude voltage is supplied to the piezoelectric actuator for the cantilever oscillation [18].

As the force sensor, we used the conductive silicon cantilever with a sharpened tip. Its spring constant and mechanical resonant frequency were 48 N/m and 160 kHz, respectively. The nominal radii of curvature for the tip apex were 5–10 nm. The silicon tip was cleaned by Ar-ion sputtering. So, there are dangling bonds out of the silicon tip apex.

The $\sqrt{3}$-Ag surface was prepared as follows: First, the Si(111)-(7×7) reconstructed [hereafter referred to as Si-(7×7)] surface was prepared with the thermal treatment of the silicon wafer. Second, silver was deposited on the Si-(7×7) surface at room temperature, and annealed [19,20].

For the $\sqrt{3}$-Ag surface, the honeycomb-chained trimer (HCT) model [21,22] was accepted as the appropriate model. As shown in Fig. 1, this structure contains the silver trimers at the topmost layer and the silicon trimers at the second layer. In this model, the silicon atoms at the second layer and the silver atoms at the topmost layer form covalent bonds, and hence the dangling bonds out of the lower silicon atoms are terminated by the
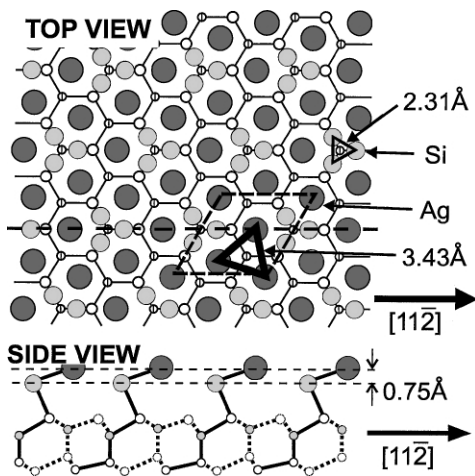
FIG. 1. The HCT model for the structure of the Si(111)-($\sqrt{3} \times \sqrt{3}$)-Ag surface. The black closed circles, gray closed circles, and open and closed circles with vertical lines indicate a silver atom at the topmost layer, silicon atom at the second layer, silicon atom at the third layer, and silicon atom at the fourth layer, respectively. Rhombus indicates $\sqrt{3} \times \sqrt{3}$ unit cell. The thick solid triangle indicates a silver trimer. The thin solid triangle indicates a silicon trimer.

topmost silver atoms. The interatomic distance between the nearest neighbor silver atoms forming silver trimer and that between lower silicon atoms forming silicon trimer in Fig. 1 are 3.43 and 2.31 Å, respectively [22]. The apexes of the silicon and silver trimers face the [$11\bar{2}$] direction and the direction tilted a little to the [$\bar{1}\bar{1}2$] direction, respectively [21]. Besides, there are three silver atoms and three silicon atoms per $\sqrt{3} \times \sqrt{3}$ unit cell.

We performed atomic scale imaging at various tip-sample distances Z on the $\sqrt{3}$-Ag surface. At the beginning of the measurement, we obtained the three types of noncontact AFM images (type-I) depending on the tip-sample distance such as reported in a previous paper [12]. When the tip further approached the $\sqrt{3}$-Ag surface, the tip accidentally contacted the $\sqrt{3}$-Ag surface. After that,

other types of noncontact AFM images (type-II) were reproducibly obtained on the $\sqrt{3}$-Ag domain, as shown in Fig. 2. Further, after we observed the Si-(7×7) domain, type-I was reproducibly obtained on the $\sqrt{3}$-Ag domain again. Similar phenomena concerning the drastic contrast change due to accidental contact were observed on the Si(100)-(2×1) reconstructed surface [23].

Figures 2(a)–2(c) show the typical atomic resolution images after the accidental contact (type-II) on $\sqrt{3}$-Ag surface measured at the frequency shift of (a) $\Delta \nu = -4.4$ Hz, (b) $\Delta \nu = -6.9$ Hz, and (c) $\Delta \nu = -9.4$ Hz, respectively. The tip-sample distances Z are roughly estimated to be $Z = 1.9$, 0.6, and ~ 0 Å (in the noncontact region), respectively. Here, the tip-sample distances Z were estimated from the distance dependence of the frequency shift $\Delta \nu$ (frequency shift curve) and the vibration amplitude of the oscillating cantilever [7]. We defined $Z = 0$, where the vibration amplitude began to decrease due to an energy loss of the oscillating cantilever. The energy loss is due to the cyclic repulsive contact between the tip and the surface or to the damping [24] of the cantilever on the surface. During noncontact AFM imaging in Fig. 2, the vibration amplitude of the cantilever did not change. The frequency shift curve without discontinuity was observed. As shown in Fig. 2, when the tip approached the surface, the image patterns have no distance dependence, and the image contrast only improves. We can observe a triangle pattern composed of three bright spots in the unit cell. The distance between the bright spots is 3.5 ± 0.2 Å. Direction of the apex of all triangles is tilted a little from the [$\bar{1}\bar{1}2$] direction.

It should be noted that this unique triangle pattern of the noncontact AFM images measured on the $\sqrt{3}$-Ag surface is not caused by tip artifacts. This reason is as follows: First, as shown in Fig. 3, we could observe atomic scale point defects on the $\sqrt{3}$-Ag surface, which means the success of the true atomic resolution imaging. Second, even using other tips, we could observe the same image pattern and the distance dependence reproducibly.
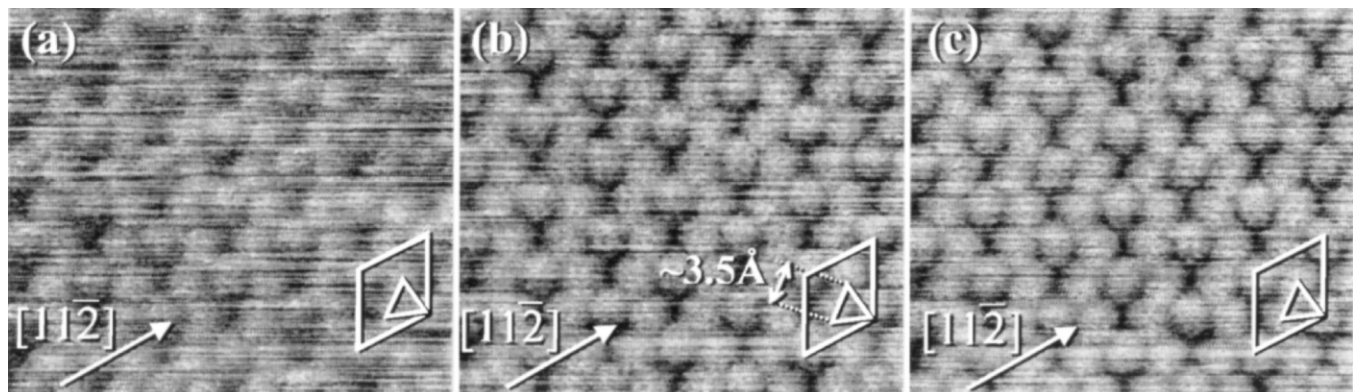
FIG. 2. Noncontact AFM images measured at the frequency shift of (a) $\Delta \nu = -4.4$ Hz, (b) $\Delta \nu = -6.9$ Hz, (c) $\Delta \nu = -9.4$ Hz on Si(111)-($\sqrt{3} \times \sqrt{3}$)-Ag surface after the accidental contact. The vibration amplitude of cantilever and scan areas are 43 Å and 38 Å $\times$ 34 Å, respectively. A rhombus indicates unit cell.
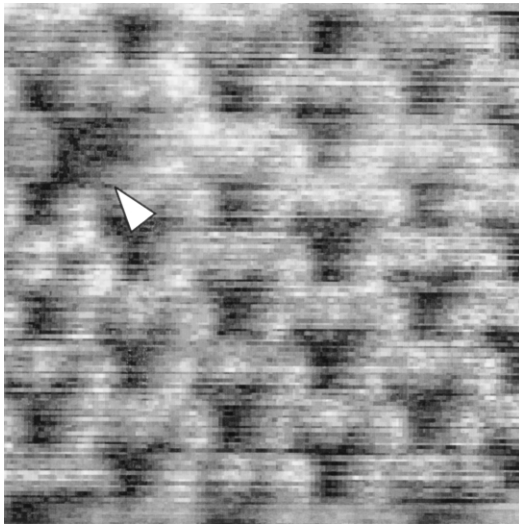
FIG. 3. Noncontact AFM image with a point defect on Si(111)-($\sqrt{3} \times \sqrt{3}$)-Ag surface. The point defect is indicated by the white arrow. The vibration amplitude of cantilever and scan areas are 43 Å and 35 Å × 35 Å, respectively.

We will now discuss the distance dependence of the image contrast measured on the $\sqrt{3}$-Ag surface. So far, on the Si(100)-(2 × 1) and the $\sqrt{3}$-Ag surfaces, the distance dependence of the image contrast has been investigated experimentally by our group [12,23]. We found that the image contrast, the imaging patterns, and distance dependence are affected by the chemical bonding interaction between the tip and the surface.

On the Si(100)-(2 × 1) surface, noncontact AFM images showed a drastic change of the contrast whether the silicon tip was inert or chemically reactive [23]. In the case of an inert silicon tip without discontinuity in the frequency shift curve, the image patterns have no distance dependence, and the noncontact AFM image almost reflected the surface topography including dimers and adsorbates. In the case of a reactive silicon tip with discontinuity in the frequency shift curve, the image patterns have strong distance dependence. Far from the surface, the noncontact AFM images reflected surface topography, but close to the surface, they strongly reflected chemical reactivity of the surface rather than surface topography [23].

On the $\sqrt{3}$-Ag surface, noncontact AFM images measured with a chemically reactive silicon tip showed the strong distance dependence of the image patterns [12]. When the silicon tip was close to the surface, the image pattern changed from the honeycomb structure to the periodic structure composed of three bright spots [12].

Thus, in the case of the chemically reactive tip, strong distance dependence of the image pattern has been observed, while in the case of the inert tip, no distance dependence has been observed. On the other hand, in the present experiment, the triangle pattern of the noncontact AFM images in Fig. 2 does not change when the AFM tip approaches the $\sqrt{3}$-Ag surface. This strongly suggests

that the strong chemical bonding interaction between the silicon tip and the surface does not contribute to image contrast and the tip apex is chemically inert.

Next, by comparing our present image pattern with the HCT model [21,22], we will consider which sites on the $\sqrt{3}$-Ag surface were observed as the triangle pattern in the noncontact AFM image of Fig. 2. There are two types of triangle structures on the surface; one is the silver trimer at the top layer, and the other is the silicon trimer at the second layer. The measured distance between the bright spots of 3.5 ± 0.2 Å agrees with the interatomic distance for the silver trimer (3.43 Å) within the experimental error, while it does not agree with that for the silicon trimer (2.31 Å). Further, the measured direction of the apex of the triangle pattern (tilted [$\bar{1}\bar{1}2$] direction) agrees with that for the silver trimer, while it does not agree with that for the silicon trimer ([$11\bar{2}$] direction). So, we conclude that the most appropriate site, which was observed as the triangle pattern in Fig. 2, is the site of individual silver atoms forming the silver trimer.

From the previous [12] and present noncontact AFM images on the $\sqrt{3}$-Ag surface, interestingly, we found that there are two different atom sites, which noncontact AFM can image just before contact on the surface, the intermediate site between silver and silicon atoms in type-I and the top site of the silver atoms in type-II. So, we will discuss the possible origin for the observation of the two different atom sites. As described above, this change of the observation site occurred after the accidental contact between the tip and the $\sqrt{3}$-Ag surface during the AFM observation. Thus, this unique phenomenon seems to have originated from the adsorption of the silver atom onto the apex of the silicon tip. Namely, the physical and/or chemical properties of the tip apex changed by the adsorption of the silver atom due to the accidental contact. Why the silver atom is adsorbed on the tip apex is as follows.

(i) Before the accidental contact, the atom of the tip apex is the silicon, because the silicon tip was cleaned *in situ* by Ar ions sputtering before AFM imaging and maintained in a vacuum condition better than 1×10^{-10} Torr. On the other hand, there are only two types of atoms (silver and silicon) on the $\sqrt{3}$-Ag surface. If a silver atom is adsorbed on the silicon tip apex, the physical and/or chemical properties of the tip apex will change strongly. If a silicon atom is absorbed on the tip apex, its properties will not change.

(ii) The change of image patterns from type-I to type-II occurred only on the $\sqrt{3}$-Ag domain during AFM imaging. It is well known that the tip readily picks up an atom from the surface [7,25]. The silicon tip would pick up the silver atom from the $\sqrt{3}$-Ag surface.

(iii) After the noncontact AFM observation on a reactive Si-(7 × 7) domain by using the type-II tip, the image patterns on $\sqrt{3}$-Ag surface were type-I. This strongly suggests that the physical and/or chemical properties of the

tip apex changed due to the observation on the Si-(7×7) domain. Namely, on the Si-(7×7) domain, the tip would drop the adsorbed silver atom onto the surface, or would pick up the silicon atom from the surface.

(iv) In the noncontact AFM observation of the surface coexisting with both Si-(7×7) and $\sqrt{3}$-Ag domains, the image pattern of type-I was obtained on the $\sqrt{3}$-Ag domain but the image pattern of type-II was not obtained. This also strongly suggests that the physical and/or chemical properties of the tip apex change on the Si-(7×7) domain, even if the tip picks up the silver atom on the $\sqrt{3}$-Ag domain.

Finally, we will consider the imaging mechanism of the individual silver atoms on the $\sqrt{3}$-Ag surface (Fig. 2; type-II) with noncontact AFM. From the above discussion, it is expected that a dangling bond out of a silicon tip apex is terminated by the silver atom, due to the adsorption of the silver atom onto the apex of a silicon tip. In this case, the tip-sample interaction contributing to the noncontact AFM imaging seems to originate from the van der Waals interaction and/or onset of the overlap of orbitals between the silver atom on the tip and the silver atom on the surface. As a result, the top site of the individual silver atoms (or nearly true topography) will appear as a bright spot, and the image pattern will not change even at a very close tip-sample distance. In order to clarify the imaging mechanism of the noncontact AFM on the $\sqrt{3}$-Ag surface, the detailed theoretical investigations, including the effect of the relaxation [26], are required.

In conclusion, we investigated the noncontact AFM imaging on the Si(111)-$(\sqrt{3} \times \sqrt{3})$-Ag surface. We obtained the individual silver atoms on the topmost layer of the surface, which show nearly true topography. The pattern of the noncontact AFM images did not change depending on the tip-sample distance. These images seem to be obtained with the silver adsorbed tip. This result suggests that noncontact AFM images drastically change depending on the atom species on the tip apex. It should be emphasized that there is a possibility of identifying or recognizing atom species on a sample surface using the noncontact AFM, if we can control an atomic species at the tip apex.

*Electronic address: kyoko@ele.eng.osaka-u.ac.jp
[1] G. Binnig, C. F. Quate, and Ch. Gerber, Phys. Rev. Lett. **56**, 930 (1986).
[2] F.-J. Giessibl, Science **267**, 68 (1995).
[3] S. Kitamura and M. Iwatsuki, Jpn. J. Appl. Phys. **34**, L145 (1995).
[4] H. Ueyama *et al.,* Jpn. J. Appl. Phys. **34**, L1086 (1995).
[5] Y. Sugawara *et al.,* Science **270**, 1646 (1995).
[6] R. Erlandsson, L. Olsson, and P. Martensson, Phys. Rev. B **54**, R8309 (1996).
[7] T. Uchihashi *et al.,* Phys. Rev. B **56**, 9834 (1997).
[8] S. Kitamura and M. Iwatsuki, Jpn. J. Appl. Phys. **35**, L668 (1996).
[9] W. Allers *et al.,* Rev. Sci. Instrum. **69**, 221 (1998).
[10] M. Bammerlin *et al.,* Appl. Phys. A **66**, S293 (1998).
[11] K. Fukui, H. Onishi, and Y. Iwasawa, Phys. Rev. Lett. **79**, 4202 (1997).
[12] T. Minobe *et al.,* Appl. Surf. Sci. **140**, 298 (1999).
[13] S. Orisaka *et al.,* Appl. Surf. Sci. **140**, 243 (1999).
[14] R. Loppacher *et al.,* Appl. Surf. Sci. **140**, 287 (1999).
[15] W. Allers *et al.,* Appl. Surf. Sci. **140**, 247 (1999).
[16] K. Yokoyama *et al.* Rev. Sci. Instrum. (to be published).
[17] T. Albrecht *et al.,* J. Appl. Phys. **69**, 668 (1991).
[18] H. Ueyama, Y. Sugawara, and S. Morita, Appl. Phys. A **66**, S295 (1998).
[19] R. J. Wilson and S. Chiang, Phys. Rev. Lett. **58**, 369 (1987).
[20] J. E. Demuth *et al.,* J. Vac. Sci. Technol. B **6**, 18 (1988).
[21] M. Katayama *et al.,* Phys. Rev. Lett. **66**, 2762 (1991).
[22] T. Takahashi and S. Nakatani, Surf. Sci. **282**, 17 (1993).
[23] T. Uchihashi *et al.,* Appl. Surf. Sci. **140**, 304 (1999).
[24] M. Bammerlin *et al.,* Probe Microsc. **1**, 3 (1997).
[25] A. Kobayashi *et al.,* Science **256**, 1724 (1993).
[26] N. Sasaki, H. Aizawa, and M. Tsukada (to be published).